Image-Based Atmospheric Corrections — Revisited and Improved

Pat S. Chavez, Jr.

Abstract

A major benefit of multitemporal, remotely sensed images is their applicability to change detection over time. Because of concerns about global and environmental change, these data are becoming increasingly more important. However, to maximize the usefulness of the data from a multitemporal point of view, an easy-to-use, cost-effective, and accurate radiometric calibration and correction procedure is needed. The atmosphere effects the radiance received at the satellite by scattering, absorbing, and refracting light; corrections for these effects, as well as for sensor gains and offsets, solar irradiance, and solar zenith angles, must be included in radiometric correction procedures that are used to convert satellite-recorded digital counts to ground reflectances. To generate acceptable radiometric correction results, a model is required that typically uses in-situ atmospheric measurements and radiative transfer code (RTC) to correct for atmospheric effects. The main disadvantage of this type of correction procedure is that it requires in-situ field measurements during each satellite overflight. This is unacceptable for many applications and is often impossible, as when using historical data or when working in very remote locations.

The optimum radiometric correction procedure is one based solely on the digital image and requiring no in-situ field measurements during the satellite overflight. The dark-object subtraction (DOS) method, a strictly image-based technique, is an attempt to achieve this ideal procedure. However, the accuracy is not acceptable for many applications, mostly because it corrects only for the additive scattering effect and not for the multiplicative transmittance effect. This paper presents an entirely image-based procedure that expands on the DOS model by including a simple multiplicative correction for the effect of atmospheric transmittance.

Two straightforward methods to derive the multiplicative transmittance-correction coefficient are presented. The COS(TZ) or COST method uses the cosine of the solar zenith angle, which, to a first order, is a good approximation of the atmospheric transmittance for the dates and sites used in this study. The default TAUs method uses the average of the transmittance values computed by using in-situ atmospheric field measurements made during seven different satellite overflights. Published and unpublished data made available for this study by Moran et al. (1992) are used, and my model results are compared with their results. The corrections generated by the entirely image-based COST model are as accurate as those generated by the models that used in-situ atmospheric field measurements and RTC software.

Introduction

Multitemporal images collected by digital multispectral imaging systems have been available for more than 20 years and have been used for various Earth-science applications, such as mapping land use, geology, forest types, etc. Multitemporal image data collected, and being collected, by various imaging systems are becoming increasingly important because of concerns about global and environmental change. A major benefit of multitemporal remotely sensed image data is its applicability to change detection (Robinove et al., 1981; Jensen and Toll, 1982; Fung, 1990; Chavez and MacKinnon, 1994). However, to maximize the benefit, change detection must be done automatically in an operational environment, and the results must be related to physical ground units. This implies an operational radiometric-correction procedure for both sensor and atmospheric effects. There are several different methods to convert the image digital counts (DCs) to reflectances. The most straightforward method converts DCs to so-called apparent or at-satellite reflectances by correcting for sensor gains, offsets, solar irradiance, and solar zenith angle (Markham and Barker, 1986; Price, 1987; Leprieur et al., 1988; Hall et al., 1988; Hall et al., 1989; Chavez, 1989; Moran et al., 1992). However, that method does not correct for atmospheric effects, which can be substantial.

The amount of electromagnetic energy sensed by an imaging system's detectors is influenced by the atmosphere. Atmospheric effects are wavelength dependent; are both additive and multiplicative in nature; and include scattering, absorption, and refraction of light (Curcio, 1961; Turner et al., 1971; Sabins, 1978; Slater et al., 1983). Various methods to remove the additive scattering component caused by path radiance have been developed, including simple image-based dark-object subtraction (DOS) techniques (Vincent, 1972; Chavez, 1975; Ahern et al., 1977; Chavez, 1988; Chavez, 1989). However, atmospheric transmittance, which has a multiplicative effect caused by both scattering and absorption, does not have an equivalently simple and straightforward correction procedure. To accurately correct for the multiplicative effect due to transmittance usually requires in-situ field measurements of atmospheric optical depth (Slater, 1985; Slater, 1988; Holm et al., 1989). A simple but accurate atmospheric correction procedure is needed, not only for operational applications but also for many research projects that use historical data sets. The full potential of historical and new data will not be realized until an accurate, easy-to-use, and cost-effective radiometric-correction procedure is developed that converts image DCs to ground reflectances.

The optimum atmospheric correction procedure would be based solely on the digital image and would require no in-situ field measurements during the satellite overflight. The DOS method, a strictly image-based technique, is an attempt toward this ideal procedure; however, the accuracy is not ac-

U.S. Geological Survey, 2255 N. Gemini Drive, Flagstaff, AZ 86001.

TABLE 1. DATES, DISTANCES, AND TOP OF THE ATMOSPHERE SOLAR SPECTRAL IRRADIANCES. DOY, DAY OF YEAR; D, EARTH-SUN DISTANCE IN ASTRONOMICAL UNITS; Eo1, 2, 3, 4 ARE LANDSAT TM BANDS 1, 2, 3, AND 4 TOP OF THE ATMOSPHERE SOLAR SPECTRAL IRRADIANCE (W M^{-2} μM^{-1}), MODIFIED TO INCLUDE THE AFFECT OF THE D * D TERM IN EQUATION 2 (MORAN, PERSONAL COMMUNICATION), FOR SEVEN SATELLITE OVERFLIGHT DATES (MORAN ET AL., 1992).

Date	DOY	D	Eo1	Eo2	Eo3	Eo4
23 Jul 85	204	1.01580	1895.1	1770.5	1497.3	1010.6
08 Aug 85	220	1.01382	1895.1	1770.5	1497.3	1010.6
27 Oct 85	300	0.99360	1980.8	1850.5	1565.0	1056.3
20 Mar 86	079	0.99608	1970.9	1841.3	1557.2	1051.0
05 Apr 86	095	1.00065	1953.0	1824.5	1543.0	1041.4
21 Apr 86	111	1.00515	1935.5	1808.2	1529.2	1032.1
24 Jun 86	175	1.01690	1891.0	1766.7	1494.1	1008.4

ceptable for many applications, especially those dealing with medium to bright reflectance values. One of the main reasons for the unacceptable accuracy is because the DOS model does not correct for the multiplicative effect of transmittance. This paper's main objective is to present an entirely image-based procedure that expands on the DOS model by including a simple multiplicative correction for transmittance. Published and unpublished data from Moran et al. (1992) were made available to the author for this study. Therefore, this paper also compares their results with results generated by the new COST and default TAUs image-based models.

Background and Data Set Used

As stated by Moran et al. (1992), "in response to the need for a simple atmospheric correction method and the consequent verification of such a method, an experiment was designed to acquire a data set suitable for testing atmospheric correction procedures under a variety of conditions." With Dr. Moran's permission, I have used the same data set in my analysis. She made available not only the data published in the paper, but also other data used to derive those shown in their tables and figures. This made the evaluation and comparison of the new image-based models easier and more complete.

To evaluate the results generated by the various models, Moran et al. used spectral data collected simultaneously by satellite, aircraft, and ground-based sensors over large uniform ground targets during multiple satellite overflights. Atmospheric optical depth measurements were also made during each satellite overflight and used as input to radiative transfer codes (RTCs) to compute surface reflectances. As expected, the results derived by using the in-situ optical depth measurements and RTC software were the most accurate. They compared these results with those generated by using simpler atmospheric correction models. Their evaluation included use of the in-situ atmospheric measurements as input to different RTCs: Herman-Browning (HBC) (Herman and Browning (1965), which gave the best results) and 5S (Tanre et al., 1990). However, as stated in their paper, "This type of procedure has been shown to be accurate by Holm et al. (1989) and Moran et al. (1990), but to expensive and time-consuming for it to be considered for use operationally."

The simpler image-based methods used by them for comparison included using (1) RTCs with simulated, rather than measured, atmospheric information and (2) the dark-object subtraction (DOS) technique (Vincent, 1972; Chavez, 1975; Chavez, 1988; Chavez, 1989). The model that used a simulated atmosphere to infer the required correction parameters was suggested by Ahern et al. (1977). The information derived by using the simulated atmosphere was used with a simple procedure based on LOWTRAN 7 (Kneizys et al., 1988), as well as with a more complex procedure based

on 5S (Tanre et al., 1990). These models corrected for both the additive scattering and the multiplicative transmittance components, while the DOS model corrected only for the additive scattering component due to path radiance. This paper presents a comparison among the results generated by (1) the in-situ atmospheric optical depth measurements RTC method (HBC, the best), (2) RTC with simulated atmosphere method (5SD), (3) the DOS method, and (4) the new COST and default TAUs entirely image-based models derived in this paper.

Moran et al. (1992) used the University of Arizona's Maricopa Agricultural Center (MAC) as their test site over which the simultaneous ground, aircraft, and satellite measurements were made (Jackson, 1990). Landsat-5 Thematic Mapper (TM) data collected during overflights from April 1985 to June 1986 were used (Moran, 1986). Twelve TM scenes were collected, but five of them were not used because of unfavorable cloudy conditions. The satellite overpass specifications for the seven dates used are shown in Table 1. The field and aircraft measurements include seven soil and seven vegetation ground targets, which are shown as separate groups in the tables and bar graphs. However, I moved the vegetation entry for 27 October 1985 (DOY 300) into the soils group because of its moderately higher reflectance values in the visible bands and lower vegetation index. These two catogories are used to generate various statistical information for comparisons throughout the paper. Table 2 shows results of the aircraft-based reflectance measurements for the various soils and vegetation targets. On the basis of earlier work, Moran et al. (1992) assumed that these values were equivalent to ground reflectances and used them to determine the accuracy of the various models (Holm et al., 1989). To make it easier to compare results, several tables and plots in this paper duplicate the information given by Moran et al. (1992). For a detailed description of the procedures used for ground, aircraft, and atmospheric measurements and complete analysis, refer to Moran et al. (1992).

Radiometric Correction Models

Generally, the objective of a radiometric atmospheric correction procedure is to convert satellite-generated digital counts (DCs) to ground reflectances (i.e., absolute surface reflectances). How the different model parameters are derived depends on the available information (i.e., ground and/or

TABLE 2. AIRCRAFT-BASED MEASURED REFLECTANCES OF MORAN ET AL. (1992). ON THE BASIS OF PREVIOUS WORK, REFLECTANCES ARE ASSUMED TO REPRESENT THE GROUND REFLECTANCES AND ARE USED TO CHECK THE ACCURACY OF THE VARIOUS MODELS. GROUND TARGETS ARE SEPARATED INTO SOILS OR VEGETATION AS THEY WERE BY MORAN ET AL. DOY, DAY OF YEAR, 1985-86.

DOY (1985-86)	TM1	TM2	TM3	TM4
		Soils		
204	0.0805	0.1205	0.1684	0.2155
220	0.0845	0.1256	0.1854	0.2250
300	0.0745	0.0941	0.1082	0.2425
300*	0.0953	0.1424	0.1947	0.2437
079	0.0698	0.1072	0.1539	0.1997
095	0.0664	0.0992	0.1498	0.2039
111	0.0924	0.1398	0.2061	0.2736
175	0.1046	0.1491	0.2101	0.2662
		Vegetation		
204	0.0232	0.0589	0.0269	0.5387
220	0.0302	0.0591	0.0365	0.5861
079	0.0260	0.0465	0.0302	0.3758
095	0.0370	0.0634	0.0533	0.4124
111	0.0235	0.0542	0.0239	0.6258
175	0.0310	0.0650	0.0336	0.5713

*Moved from vegetation section.

atmospheric *in-situ* measurements or lack thereof). Regardless of the model, though, DCs must first be converted to at-satellite radiances by removing the gain and offset effects introduced by the imaging system. If the data have been processed to remove striping noise by using a statistical technique, these additional gains and offsets must also be included in the correction. The gain and offset values used for these particular data are given in Moran *et al.* (1992, p. 175) and are not duplicated here. The equation to convert satellite DCs to at-satellite radiances is

$$\text{Lsat} = (\text{DC} - \text{Offset})/\text{Gain} \qquad (1)$$

where Lsat is the at-satellite spectral radiance for the given spectral band (W m^{-2} sr^{-1} μm^{-1}), DC is the digital count at the given pixel for the given spectral band, Offset is the offset for the given spectral band (DC), and Gain is the gain for the given spectral band (DC m^2 sr μm W^{-1}).

Next, at-satellite radiances must be converted to surface reflectances by correcting for both solar and atmospheric effects. The general model/equation used to do this and presented as Equation 3 by Moran *et al.* (1992, p. 172) is

$$\text{REF} = \frac{(\text{PI} * (\text{Lsat} - \text{Lhaze}))}{(\text{TAUv} * (\text{Eo} * \text{Cos}(\text{TZ}) * \text{TAUz} + \text{Edown}))} \qquad (2)$$

The definitions are those given by Moran *et al.* (1992): i.e.,

REF = Spectral reflectance of the surface.
Lhaze = Upwelling atmospheric spectral radiance scattered in the direction of and at the sensor entrance pupil and within the sensor's field of view (W m^{-2} sr^{-1} μm^{-1}), i.e., the path radiance.
TAUv = Atmospheric transmittance along the path from the ground surface to the sensor.
Eo = Solar spectral irradiance on a surface perpendicular to the sun's rays outside the atmosphere (W m^{-2} μm^{-1}). Eo contains the Earth-sun distance term (D*D) imbedded and is in astronomical units (AUs are a function of time of year and range from about 0.983 to 1.017).
TZ = Angle of incidence of the direct solar flux onto the Earth's surface (solar zenith angle, Thetaz).
TAUz = Atmospheric transmittance along the path from the sun to the ground surface.
Edown = Downwelling spectral irradiance at the surface due to scattered solar flux in the atmosphere (W m^{-2} μm^{-1}).

All the radiometric correction procedures below start with this general model (Equation 2) but make different simplifying assumptions that eliminate certain parameters. The information available about the data and atmospheric conditions determines what assumptions must be made and, therefore, the specific model that is to be used. Often, the method used to derive the required parameters can also determine assumptions that must be made.

Apparent Reflectance Model
The apparent reflectance model is the simplest one used to convert at-satellite radiances to reflectances. It corrects for spectral band solar irradiance and solar zenith angle of the image but makes no attempt to correct for atmospheric scattering and absorption. For the apparent reflectance model, the following applies in Equation 2:

TAUz = 1.0 (ignores atmospheric transmittance),
TAUv = 1.0 (ignores atmospheric transmittance),
Edown = 0.0 (ignores downwelling), and
Lhaze = 0.0 (ignores scattering due to path radiance).

The main advantange of this model is that it is very simple and easy to apply; it does not require *in-situ* field measurements of ground reflectances and/or atmospheric optical depths or simulated atmospheric parameters. The disadvantages are that the accuracy is usually not acceptable for many applications, especially for TM bands 1 and 4 (Moran *et al.*, 1992), and the correction is based on the sensor's gain and offset values, which are uncertain due to changing sensor characteristics (Slater *et al.*, 1987; Thome *et al.*, 1993; Moran *et al.*, in press). This second disadvantage is one that exists for all the models considered in this paper and should be kept in mind by the reader.

DOS Model
The image-based dark-object subtraction (DOS) model used in the comparison by Moran *et al.* (1992) is the one discussed in several previous papers (Vincent, 1972; Chavez, 1975; Chavez, 1988; Chavez, 1989). The basic assumption is that within the image some pixels are in complete shadow and their radiances received at the satellite are due to atmospheric scattering (path radiance). This assumption is combined with the fact that very few targets on the Earth's surface are absolute black, so an assumed one-percent minimum reflectance is better than zero percent. The paper by Chavez (1989) discusses an improved method of selecting the dark-object haze values for the separate spectral bands. The objective of that improved dark-object method is to select spectral-band haze values that are correlated to each other, rather than by using the histograms of each spectral band independently, which can cause haze-selection problems when topographic/shadow conditions are minimal. Both methods generate haze values that are very similar when sufficient topography exists, as in the images used for this study. The histogram and DOS one-percent haze-selection method was used by Moran *et al.* (1992); therefore, it is the one compared in this paper.

Besides correcting for the same parameters that the apparent reflectance model does, the image-based DOS radiometric correction model also corrects for the atmospheric additive scattering component attributed to the path radiance. Therefore, in the general radiance-to-reflectance model shown in Equation 2, the following applies for the DOS model:

TAUz = 1.0 (ignores atmospheric transmittance),
TAUv = 1.0 (ignores atmospheric transmittance),
Edown = 0.0 (ignores downwelling), and
Lhaze = value derived from the digital image using the dark-object criteria.

The DOS model's main advantages are that it is strictly an image-based procedure and does not require *in-situ* field measurements and that it is simple and relatively straightforward to apply. The main disadvantages are that for reflectance values greater than about 15 percent the accuracy is often not acceptable and that the selection of the haze values must be done with care.

Moran *et al.* Models
The evaluation by Moran *et al.* (1992) examined several different models to derive the atmospheric parameters needed for Equation 2. These models included using RTC solutions generated by using both *in-situ* measured (HBC and 5S) or simulated (LOWTRAN 7 and 5S) atmospheric information. The comparisons in this paper are limited to the uncorrected/apparent, DOS 1-percent, HBC (which gave the best results), and simulated 5S models, and the new entirely image-based models derived in this paper. As expected, the most accurate model in the Moran *et al.* (1992) study was the one that used *in-situ* atmospheric measurements, made during the satellite

TABLE 3. SOLAR ZENITH ANGLES, THEIR COSINES, DEL VALUES, AND COMPUTED TAUz VALUES FOR TM BANDS 1, 2, 3, AND 4 FOR THE 1985-86 OVERFLIGHT DATES. DOY, DAY OF YEAR FOR SATELLITE OVERFLIGHT-IMAGE DATE; THETAZ (TZ), SOLAR ZENITH ANGLE; COS(TZ), COSINE OF THETAZ; DEL, OPTICAL DEPTH VALUES COLLECTED BY MORAN ET AL.; TAUz, MULTIPLICATIVE TAUz VALUES; Ave, AVERAGE TAUz VALUES. TAUz VALUES WERE COMPUTED USING THE OPTICAL DEPTH MEASUREMENTS GIVEN BY MORAN ET AL. FUNCTION USED TO COMPUTE TAUz WAS EQUAL TO EXP(−DEL * SEC(THETAZ)), WHERE DEL IS EQUAL TO OPTICAL DEPTH, EQUATION 3.

DOY	THETAZ	COS(TZ)	de11/TAUz1	de12/TAUz2	de13/TAUz3	de14/TAUz4	Ave, TAUz
204	29.84	0.87	0.29/0.71	0.22/0.78	0.14/0.85	0.07/0.92	0.82
220	30.08	0.87	0.33/0.68	0.22/0.78	0.16/0.83	0.10/0.89	0.80
300	50.88	0.63	0.29/0.64	0.20/0.73	0.13/0.81	0.07/0.89	0.77
079	43.76	0.72	0.25/0.71	0.18/0.78	0.11/0.86	0.05/0.93	0.82
095	38.35	0.78	0.25/0.72	0.20/0.77	0.12/0.86	0.06/0.93	0.82
111	33.35	0.84	0.21/0.78	0.13/0.86	0.09/0.90	0.05/0.94	0.87
175	27.56	0.89	0.33/0.69	0.22/0.78	0.15/0.84	0.09/0.90	0.80
Ave.		0.80	0.70	0.78	0.85	0.91	0.81

Note: Table 3 shows that, to a first order, cosine(thetaz) is equal to the TAUz value of the individual spectral bands. Average values were computed to show possible default values for each spectral band; these are the values used by the default TAUs model. The del values are rounded off to two places, but the actual computations were done using four place accuracy.

overflights, which included optical depths as input to RTC software to compute the relation between surface reflectance and sensor radiance (Moran *et al.*, 1992, p. 170). However, acceptable results were also generated with the model that used simulated atmosphere parameters as input to RTC software. A main difference between the models using RTC software and the DOS method was that *in-situ* measurements or simulated atmospheres were used to derive the required atmospheric parameters for Equation 2, including corrections for transmittance and downwelling. In the general radiance-to-reflectance model shown in Equation 2, the following criteria apply:

$$TAUz = EXP(-del * sec(TZ)) \tag{3}$$

and

$$TAUv = EXP(-del * sec(TV)) \tag{4}$$

where EXP is the exponential, sec is the secant, del is the optical thickness values measured *in-situ* at the given wavelengths, TZ is the solar zenith angle, thetaz, and TV is the viewing angle (zero degrees for nadir viewing systems, thetav). Edown is derived from atmospheric measurements made *in-situ* or computed from simulated atmospheres, and Lhaze is derived from atmospheric measurements made *in-situ*, or simulated atmosphere, or by using the DOS Lhaze procedure.

The advantage of the RTC-driven models was the improved accuracy. The procedure that used simulated atmospheres rather than *in-situ* measurements had the added advantage of not requiring someone to be in the field during the satellite overflight. However, it did require use of the RTC software. The HBC model generated the best results but required *in-situ* measurements and, therefore, someone in the field during each of the satellite overflights.

Improved Image-Based Model

The improvement made to the image-based DOS model is based on a method that derives a correction for the multiplicative transmittance effect by using one of two techniques. Equation 2 shows that the error for not including a multiplicative correction for transmittance is approximately 1.0/(TAUz * TAUv) which, for the seven dates used, implies an approximate overall error of 30 percent. Therefore, a correction for the multiplicative transmittance component can substantially improve the DOS model results. In this study two different methods were used to derive the required TAU values in Equation 2. Both methods that correct for multiplicative transmittance effects are independent of *in-situ* atmospheric and ground measurements. Field-independent derived TAU values were used, along with the DOS Lhaze additive-scattering component due to path radiance, in the gen-

eral radiance-to-reflectance model (Equation 2) to compute surface reflectances.

The first method used to derive TAU values independent of *in-situ* field measurements is very straightforward. As given by Moran *et al.* (1992, p. 172), the multiplicative transmittance component for scattering and weak absorption is approximated by Equations 3 and 4 (repeated below):

$$TAUz = EXP(-del * sec(TZ)) \tag{3}$$

and

$$TAUv = EXP(-del * sec(TV)) \tag{4}$$

where del is the optical thickness values at given wavelengths, TZ is the solar zenith angle (thetaz), and TV is the viewing angle (zero degrees for Landsat TM images — thetav).

Using the spectral optical depth and solar zenith values given by Moran *et al.* (1992, p. 174), the TAUz values were computed for TM bands 1, 2, 3, and 4. Table 3 shows the computed TAUz values, along with solar zenith angles and their cosines for the seven satellite overflight dates. Empirically, the values in Table 3 show that, to a first order, the cosine of the solar zenith angle is a good approximation of TAUz. It approximates TM bands 1 and 2 best in some cases and TM bands 3 and 4 best in others. However, the average TAUz of all bands for all dates is very similar to the average of the cosine values (0.81 and 0.80, respectively). Equation 3 shows that transmittance is a function of the solar zenith angle (TZ) and the optical depth (del). For most acceptable images, TZ is in the range of 30 to 55 degrees and del has a range of 0.08 to 0.30. Therefore, in the EXP(−del * sec(TZ)) function, the variation of sec(TZ) is about 2.7 times larger than that for del, which implies that TZ (the solar zenith angle) is the more dominant variable. So, a relation that is strictly dependent on TZ to approximate the exponential function, to a first order, may be acceptable (i.e., set it equal to the cosine of TZ). This empirically observed relation was used as the first method to select TAUz values.

To help strengthen this empirically observed relation seen in Table 3 between the cosine of the solar zenith angle (TZ) and EXP(−del*sec(TZ)), the power series expansion of these two functions was used. The first four terms of the power series are

$$Cos(TZ) = 1 - TZ^2/2! + TZ^4/4! - TZ^6/6! \tag{5}$$

and

$$EXP(-del*sec(TZ)) = 1 - del*sec(TZ) + (del^2)*(sec(TZ)^2)/2! - (del^3)*(sec(TZ)^3)/3! \tag{6}$$

The solar zenith angle TZ is in radians and ! represents fac-

toral; the power series expansions were done using the standard Taylor series equations (Boas, 1966, p. 19). The average TZ and del values for the seven dates used are 0.64 and 0.17, respectively. Using these two average values in the power series expansions generates values of 0.8021 for the cosine and 0.8087 for the exponential when carried out four terms; if only the first two terms are used, the cosine value is 0.7952 and the exponential value is 0.7882 (both are within one percent of each other). As in Table 3, these calculations also shows that, to a first order, the cosine of the solar zenith angle and the exponential of minus del times the secant of the solar zenith angle are equal for these data.

As will be shown in the results section, using the cosine of the solar zenith angle for TAUz substantially improves the DOS results, and, in fact, the results are as good as those generated by the HBC model. I call the cosine of the solar zenith angle, cos(TZ), correction the COST model.

Because the cosine is independent of wavelength, an alternative default method, one dependent on wavelength, was also developed for comparison. It is also quite simple, straightforward, and entirely image based. The alternative method simply uses default TAUz values, which are the average for each spectral band using the seven dates given by the Moran et al. (1992) data. These default values for TM bands 1, 2, 3, and 4 are the averages given in Table 3. I refer to this correction as the default (DEF) TAUs model and can be used instead of the COST model when information on a per image basis is not available. In the general radiance-to-reflectance model shown in Equation 2, the following criteria apply:

TAUz = Cos(thetaz) for the COST model
or
TAUz = Default TAUz values from Table 3 for the DEF TAUs model; 0.70, 0.78, 0.85, and 0.91 for TM bands 1, 2, 3, and 4, respectively;
TAUv = Cos(thetav) = 1.0 because thetav is zero degrees for nadir view;
Edown = 0.0 (ignores downwelling); and
Lhaze = Value derived from the digital image using the dark-object criteria (identical to the DOS model).

As in the DOS model, the main advantages of these models are that they are strictly image-based procedures and therefore do not require in-situ field measurements and they are simple and very straightforward to apply. Compared to that of the DOS model, the accuracy generated by both the COST and DEF TAUs image-based models is substantially improved, and use of RTC software is not required. However, as for the DOS model, a disadvantage is that the dark object DN value for Lhaze must be selected carefully.

Results and Discussions
This section compares the aircraft-based measured reflectances, which are used by Moran et al. (1992) as equivalent ground reflectances based on previous research (Holm et al., 1989), with the computed values generated by the various models. As done by Moran et al., the results are compared in table, plot, and bar-graph format. The tables show the differences between the computed reflectance values and the aircraft-based ground-measured values, as well as the average of the absolute value of these differences for each spectral band on each satellite overflight date. Note that these comparisons differ slightly from those made in several graphs presented by Moran et al. (1992). Several of their graphs show the average of the difference, not of the absolute value of the difference. The absolute-value method emphasizes the amplitude of the error rather than whether the overall results are over or under corrected, and it keeps positive and negative errors from canceling each other out. For example, the uncorrected/apparent reflectance model generates results that are over

corrected for dark reflectances and under corrected for bright reflectances, while the DOS model tends to under correct most of the reflectances (see Figure 1). Therefore, the apparent reflectance model has a larger number of negative and positive errors that cancel each other out compared to the DOS model. Because the question of over or under correction is important, the tables show differences between the computed and measured values for each band on every date in positive and negative format. The graphs show the scatter plots of all the measured versus computed values for each model and show whether the data are being over or under corrected (see Figures 1 and 2).

Table 2 shows the aircraft-based measured-reflectance values that Moran et al. (1992, p. 174) considered to be the correct ground readings. As in Moran et al. (1992), this paper maintains the same groups of soils and vegetation except, as noted earlier, the vegetation entry for DOY 300 was moved into the soils group because both the moderately high reflectance values in the visible bands and the lower vegetation index imply a soils target. In TM bands 1, 2, and 3 (visible bands), the reflectances of these two groups also correspond closely to dark versus bright reflectances. Besides the computed reflectance values for the given model, each table shows the difference between the computed and the measured (Table 2) values. In these tables, positive implies over corrected and negative implies under corrected results for the following models:

Table 4, Uncorrected/apparent reflectance
Table 5, DOS 1-percent reflectance
Table 6, 5SD reflectance
Table 7, HBC reflectance
Table 8, COST reflectance
Table 9, Default TAUz reflectance

Tables 4, 5, 6, and 7 give the results generated by Moran et al. (1992); Tables 8 and 9 show the results generated by the new COST and default TAUs image-based models. The tables can be used to make very detailed comparisons between the various models. Scatter plots like those used by Moran et al. (1992) are also shown for general comparisons (Figures 1 and 2). The plots in Figure 1 are identical to those published by Moran et al. (1992). The HBC model used the in-situ atmospheric measurements as input to RTC software and, as expected, generated the best results. The 5SD model, which used simulated atmospheric information as input to RTC software, also generated acceptable results, but the DOS 1-percent model was good only for the darker reflectances. The scatter plots in Figure 2 show the results of the improved image-based models that derive the multiplicative transmittance correction coefficient by using either the cosine of the solar zenith angle (COST) or the default TAUz values (DEF TAUz). From the scatter plots and from Tables 8 and 9, we can see that the two new models have substantially improved on the DOS results; in fact, the COST model generated results as good as the HBC (best) model. The default TAUz model also improved the DOS results, but not as much as the COST model.

The two sets of bar graphs in Figure 3 compare the reflectance accuracy of each model for each spectral band for the soils group and for the vegetation group. Generally, this is a bright and dark reflectance comparison except for the near-infrared TM band 4 where vegetation reflectance values are high. For each model, the graphs show the absolute difference between the computed and measured reflectances for each individual band as well as the average of all the TM bands. This allows a comparison of not only the overall accuracy of each of the models, but also the accuracy within individual TM bands for the two data groups. For soils, which have mostly mid to high reflectance values, both the COST and default TAUz models improve on all the DOS re-
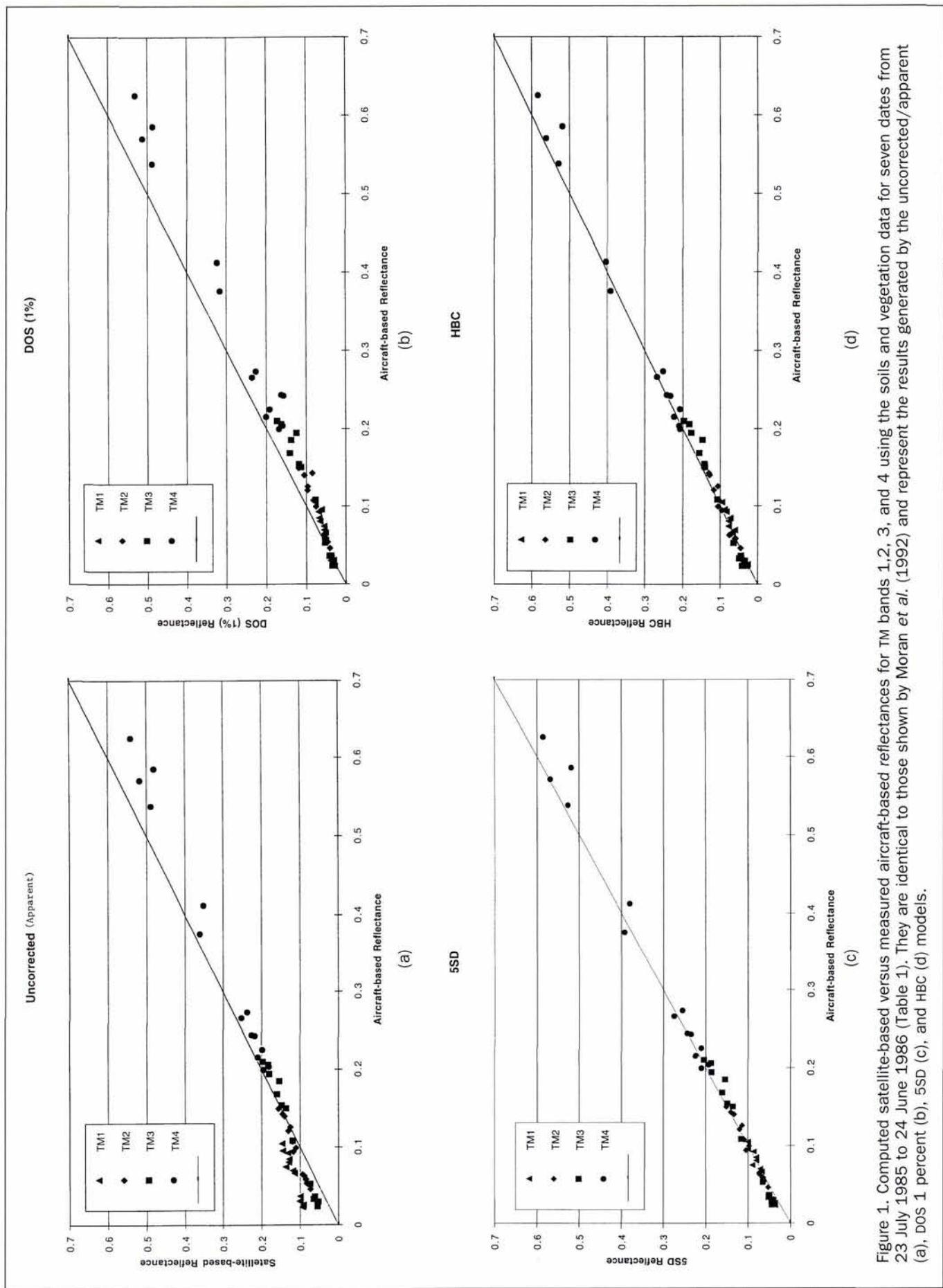
Figure 1. Computed satellite-based versus measured aircraft-based reflectances for TM bands 1, 2, 3, and 4 using the soils and vegetation data for seven dates from 23 July 1985 to 24 June 1986 (Table 1). They are identical to those shown by Moran et al. (1992) and represent the results generated by the uncorrected/apparent (a), DOS 1 percent (b), 5SD (c), and HBC (d) models.
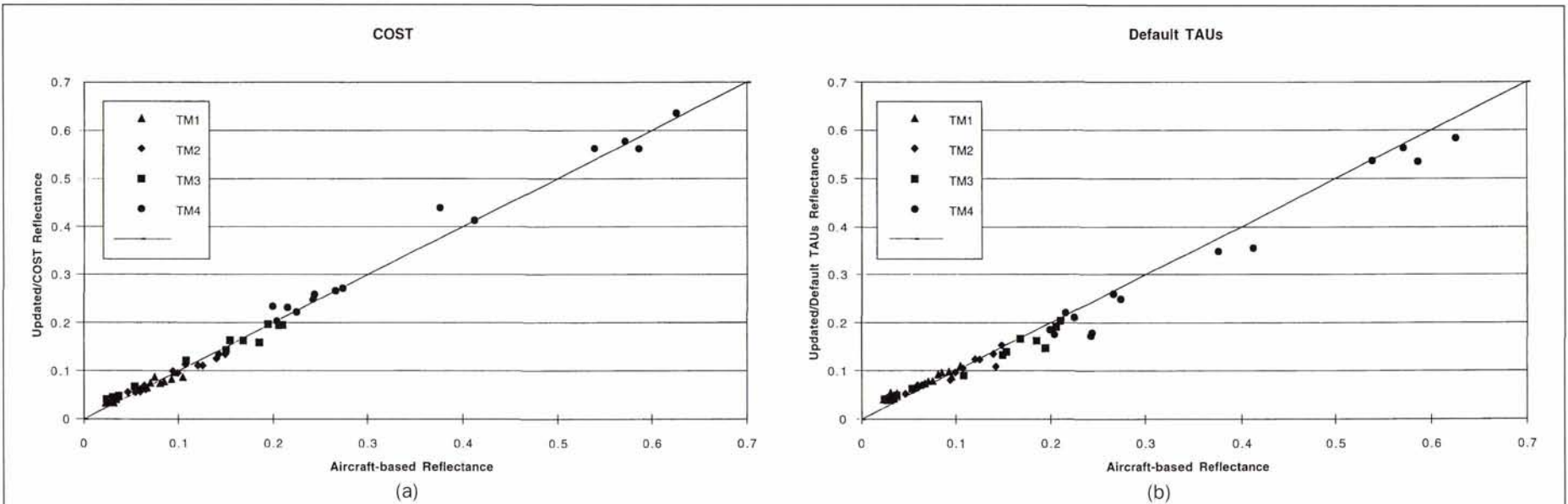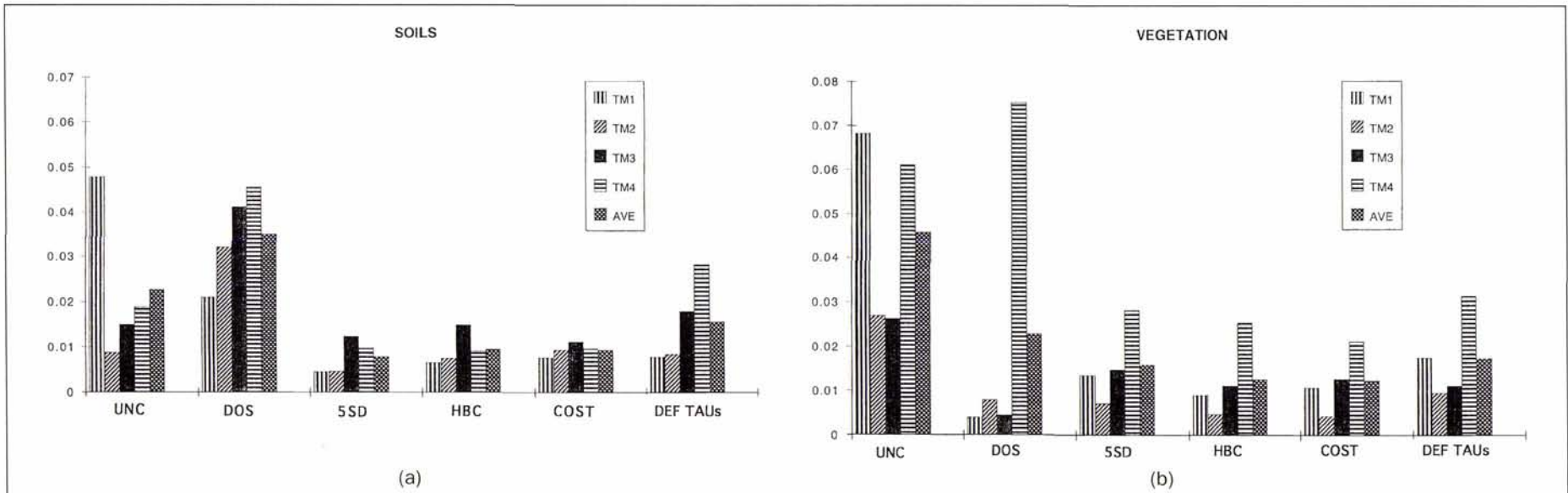
Figure 2. Results generated by the COST (a) and default TAUZ (b) models on computed satellite-based versus measured aircraft-based reflectances for TM bands 1, 2, 3, and 4 using the soils and vegetation data for seven dates from 23 July 1985 to 24 June 1986 (Table 1).

Figure 3. Reflectance results for spectral-bands TM 1, 2, 3, and 4 and an overall average, as determined by six models for the soils (a) and vegetation (b) targets. The average of the absolute difference between the computed and aircraft-based measured values are plotted.

TABLE 4. COMPUTED REFLECTANCES GENERATED BY USING THE SATELLITE UNCORRECTED/APPARENT REFLECTANCE MODEL (MORAN ET AL., 1992), THE DIFFERENCES BETWEEN THE COMPUTED AND AIRCRAFT-BASED GROUND-MEASURED VALUES, AND THE AVERAGE OF THE ABSOLUTE DIFFERENCE BETWEEN THESE VALUES. DOY, DAY OF YEAR; AVE, AVERAGE; DIFF, DIFFERENCE.

DOY	TM1	TM2	TM3	TM4	Ave/Diff/
			Soils		
204	0.1293	0.1307	0.1603	0.2098	
Diff	0.0488	0.0102	−0.0081	−0.0057	0.0182
220	0.1281	0.1255	0.1539	0.1986	
Diff	0.0436	−0.0001	−0.0315	−0.0264	0.0254
300	0.1370	0.1176	0.1195	0.2175	
Diff	0.0625	0.0235	0.0113	−0.0250	0.0306
300*	0.1449	0.1457	0.1804	0.2253	
Diff	0.0496	0.0033	−0.0143	−0.0184	0.0214
079	0.1189	0.1199	0.1481	0.1956	
Diff	0.0491	0.0127	−0.0058	−0.0041	0.0179
095	0.1147	0.1110	0.1367	0.1811	
Diff	0.0483	0.0118	−0.0131	−0.0228	0.0240
111	0.1319	0.1411	0.1829	0.2380	
Diff	0.0395	0.0013	−0.0232	−0.0356	0.0249
175	0.1467	0.1564	0.1971	0.2525	
Diff	0.0421	0.0073	−0.0130	−0.0137	0.0190
Ave/Diff/	0.0479	0.0088	0.0150	0.0189	0.0227
			Vegetation		
204	0.0940	0.0851	0.0548	0.4888	
Diff	0.0708	0.0262	0.0279	−0.0499	0.0437
220	0.0999	0.0848	0.0615	0.4811	
Diff	0.0697	0.0257	0.0250	−0.1050	0.0564
079	0.0919	0.0734	0.0523	0.3618	
Diff	0.0659	0.0269	0.0221	−0.0140	0.0322
095	0.0999	0.0896	0.0742	0.3522	
Diff	0.0629	0.0262	0.0209	−0.0602	0.0426
111	0.0925	0.0827	0.0547	0.5418	
Diff	0.0690	0.0285	0.0308	−0.0840	0.0531
175	0.1013	0.0937	0.0648	0.5179	
Diff	0.0703	0.0287	0.0312	−0.0534	0.0459
Ave/Diff/	0.0682	0.0270	0.0263	0.0611	0.0457

*Moved from vegetation section.

sults. In fact, the COST model does as well as or slightly better than the HBC model. The default TAUz model still has a problem with the near-infrared TM band 4 but does improve on the DOS model; the visible bands have acceptable accuracy, and results are similar to those generated by the COST and HBC models. In general, the DOS model has a problem with the bright soils, and results are better than the uncorrected results for only TM band 1 (as stated by Moran et al. (1992)). As shown later, this is not the case for the dark/vegetation targets. Notice that the shape of the bar graphs for models 5SD, HBC, and COST are similar.

The vegetation reflectance bar graphs, which for the visible bands represents mostly very low reflectance values, also show that the COST model generates results similar to those of the HBC model; in fact, the overall average is better because of improved results for TM bands 2 and 4. The default TAUz model generates acceptable results for the visible bands, but, like all the other models, the near-infrared band has larger errors. It is not clear why the near-infrared/TM band 4 consistently has larger errors in all the models for the vegetation group. Part of the reason may be that the multiplicative correction does not fully account for the absorption effect in the near-infrared band as well as the visible bands. However, a second possible explanation is that it is more difficult to get a good sampling of the ground when vegetation is present, compared to when the soils are bare. Therefore, the aircraft-based ground measurements of vegetated targets could have a larger error than the soils targets.

One reason it would be more noticeable in the near-infrared band, and show up as a larger error in TM band 4, is be-

cause the reflectance of vegetation in an agricultural environment can be much higher than the background soils, so an error in ground sampling would be more pronounced. In the visible bands the error would not be as noticeable because the reflectance level of vegetation is more similar to the background soils. In a previous paper it was shown that in densely vegetated areas the near-infrared band generally has more spatial variability than do the visible bands (Chavez, 1992); therefore, it may be more difficult to accurately sample vegetated targets.

One thing that stands out from the vegetation bar graphs is the fact that the DOS model does better than any of the others, including both the HBC and the COST models, for the visible bands (TM bands 1, 2, and 3). However, it does poorly on TM band 4, as stated by Moran et al. (1992), which can be due to several reasons, including (1) the lack of a transmittance correction in the model, (2) possible aircraft-based reflectance measurement errors, and (3) the fact that TM band-4 reflectance values for vegetation are quite high, so we are seeing a bright, not dark, target error condition. The similar shapes of the bar graphs for 5SD, HBC, and COST imply that errors remaining in these three models are similar (i.e., they are all correcting for the same errors, and errors that are left are common to all three models).

Several additional points should be made on the basis of the data and the results seen in this study.

(1) The cosine-derived TAUz values are a function of time of year but are independent of wavelength, while the default TAUz values are a function of wavelength but independent of time of year. The TAUz values in Table 3 show larger differences in functions of wavelength than of time of year;

TABLE 5. COMPUTED REFLECTANCES GENERATED BY USING THE IMAGE-BASED DOS 1-PERCENT MODEL (MORAN ET AL., 1992), THE DIFFERENCES BETWEEN THE COMPUTED AND AIRCRAFT-BASED GROUND-MEASURED VALUES, AND THE AVERAGE OF THE ABSOLUTE DIFFERENCE BETWEEN THESE VALUES. DOY, DAY OF YEAR, 1985-86; AVE, AVERAGE; DIFF, DIFFERENCE.

DOY(1985-86)	TM1	TM2	TM3	TM4	Ave/Diff/
204	0.0648	0.0966	0.1414	0.2008	
Diff	−0.0157	−0.0239	−0.0270	−0.0147	0.0203
220	0.0674	0.0962	0.1379	0.1920	
Diff	−0.0171	−0.0294	−0.0475	−0.0330	0.0318
300	0.0550	0.0627	0.0767	0.1570	
Diff	−0.0195	−0.0314	−0.0315	−0.0855	0.0420
300*	0.0612	0.0847	0.1244	0.1632	
Diff	−0.0341	−0.0577	−0.0703	−0.0805	0.0607
079	0.0544	0.0818	0.1182	0.1688	
Diff	−0.0154	−0.0254	−0.0357	−0.0309	0.0269
095	0.0513	0.0750	0.1128	0.1596	
Diff	−0.0151	−0.0242	−0.0370	−0.0443	0.0302
111	0.0688	0.1050	0.1627	0.2271	
Diff	−0.0236	−0.0348	−0.0434	−0.0465	0.0371
175	0.0770	0.1194	0.1733	0.2364	
Diff	−0.0276	−0.0297	−0.0368	−0.0298	0.0310
Ave/Diff/	0.0210	0.0321	0.0412	0.0457	0.0350
			Vegetation		
204	0.0285	0.0497	0.0329	0.4880	
Diff	0.0053	−0.0092	0.0060	−0.0507	0.0178
220	0.0380	0.0538	0.0416	0.4865	
Diff	0.0078	−0.0053	0.0051	−0.0996	0.0295
079	0.0303	0.0403	0.0328	0.3170	
Diff	0.0043	−0.0062	0.0026	−0.0588	0.0180
095	0.0371	0.0545	0.0528	0.3237	
Diff	0.0001	−0.0089	−0.0005	−0.0887	0.0246
111	0.0294	0.0465	0.0345	0.5309	
Diff	0.0059	−0.0077	0.0106	−0.0949	0.0298
175	0.0298	0.0541	0.0356	0.5126	
Diff	−0.0012	−0.0109	0.0020	−0.0587	0.0182
Ave/Diff/	0.0041	0.0080	0.0045	0.0753	0.0230

*Moved from vegetation section.

TABLE 6. COMPUTED REFLECTANCES GENERATED BY USING THE 5SD MODEL BASED ON A SIMULATED ATMOSPHERE AND DARK OBJECT OF 1 PERCENT (MORAN ET AL., 1992), THE DIFFERENCES BETWEEN THE COMPUTED AND AIRCRAFT-BASED GROUND-MEASURED VALUES, AND THE AVERAGE OF THE ABSOLUTE DIFFERENCE BETWEEN THESE VALUES. DOY, DAY OF YEAR, 1985-86; AVE, AVERAGE; DIFF, DIFFERENCE.

DOY	TM1	TM2	TM3	TM4	Ave/Diff/
204	0.0810	0.1200	0.1610	0.2240	
Diff	0.0005	−0.0005	−0.0074	0.0085	0.0042
220	0.0810	0.1140	0.1540	0.2110	
Diff	−0.0035	−0.0116	−0.0314	−0.0140	0.0151
300	0.0900	0.1050	0.1160	0.2350	
Diff	0.0155	0.0109	0.0078	−0.0075	0.0104
300*	0.1000	0.1400	0.1860	0.2440	
Diff	0.0047	−0.0024	−0.0087	0.0003	0.0040
079	0.0710	0.1090	0.1490	0.2100	
Diff	0.0012	0.0018	−0.0049	0.0103	0.0046
095	0.0670	0.0980	0.1360	0.1930	
Diff	0.0006	−0.0012	−0.0138	−0.0109	0.0066
111	0.0870	0.1330	0.1870	0.2550	
Diff	0.0054	−0.0068	−0.0191	−0.0186	0.0125
175	0.1000	0.1510	0.2040	0.2750	
Diff	−0.0046	0.0019	−0.0061	0.0088	0.0054
Ave/Diff/	0.0045	0.0046	0.0124	0.0099	0.0079
Vegetation					
204	0.0360	0.0640	0.0440	0.5270	
Diff	0.0128	0.0051	0.0171	−0.0117	0.0117
220	0.0460	0.0660	0.0500	0.5190	
Diff	0.0158	0.0069	0.0135	−0.0671	0.0258
079	0.0370	0.0520	0.0400	0.3930	
Diff	0.0110	0.0055	0.0098	0.0172	0.0109
095	0.0490	0.0730	0.0650	0.3810	
Diff	0.0120	0.0096	0.0117	−0.0314	0.0162
111	0.0390	0.0620	0.0430	0.5690	
Diff	0.0155	0.0078	0.0191	0.0398	0.0206
175	0.0450	0.0730	0.0510	0.5690	
Diff	0.0140	0.0080	0.0174	−0.0023	0.0104
Ave/Diff/	0.0135	0.0072	0.0148	0.0283	0.0159

*Moved from vegetation section.

however, on an overall average, the cosine function did a good job representing the TAUz values for these data (0.80 average cosine value versus 0.81 average TAUz value). On the basis of TAUz values in Table 3, it appears that the cosine model will generally undercorrect TM band 1 and overcorrect TM band 4. Even though these data cover a semi-arid environment, the cosine function and default TAUz values computed from these data may also satisfactorily approximate, to a first order, the transmittance TAUz values for continental and maritime atmospheres. Gilabert et al. (1994, Figure 3 on page 2076) show the atmospheric transmittance values for eight continental and four maritime atmospheres corresponding to their Landsat TM data. The transmittance values for TM band 1 for all 12 image dates range from 0.68 to 0.82, and continue to increase to approximately 0.95 at the longer near-infrared wavelength (p. 2074). In comparison, the transmittance values for TM band 1 for the data used in this study (Table 3) range from 0.64 to 0.78; values also increase at the longer wavelengths. The range of the cosine of the solar zenith angles for these same data — 0.63 to 0.89 — implies that the improved image-based models may also be applicable under different atmospheric conditions and nonarid environments. Further testing is required to see how well the relation actually does hold up under different conditions.

(2) Observe the relative amounts of correction contributed by the additive versus multiplicative parameters. The TAUz values in Table 3 show the amount of correction needed for each spectral band owing to multiplicative transmittance effects. By analyzing and comparing the amounts of correction generated by the additive Lhaze and the multiplicative TAUz parameters, we can see several things. First, both the additive and multiplicative corrections are larger for the visible bands than for the near-infrared band. Second, for

lower reflectances in the visible TM band 1, the additive correction is more important than the multiplicative correction. Third, for high reflectances in TM band 1, the multiplicative correction becomes more important; therefore, the additive scattering component is not always the most important correction for visible bands as indicated in previous studies (Turner et al., 1971; Slater, 1980). A similar relation exists for the near-infrared TM band 4, but the differences are not as dramatic. These differences probably are part of the explanation of why the DOS model is actually the best for very dark vegetated targets but generates unacceptable results for bright targets.

As an example, examine what happens to ground reflectance targets having 10 and 35 percent reflectance values. In TM band 1 the average additive scattering correction (Lhaze) for all seven dates is equal to about 7.8 percent reflectance. The average TAUz value of 0.70 generates a multiplicative correction of about 3 percent reflectance for the 10 percent reflectance target; it took the additive corrected 7 percent value to 10 percent (7/0.7 equals 10). However, for the 35 percent reflectance target, the TM band 1 additive correction is still 7.8 percent reflectance, but the multiplicative correction is now 10.5 percent reflectance (24.5/0.7 equals 35). The additive correction amount remains the same (7.8), while the multiplicative amount increases by a factor of 3.5 (3 to 10.5). In the near-infrared TM band 4, the average additive scattering correction (Lhaze) for all seven dates is equal to 1.75 percent reflectance. The average TAUz value of 0.91 generates a multiplicative correction of about 0.9 percent reflectance for the 10 percent reflectance target (9.1/0.91 equals 10). For the 35 percent reflectance target, the additive correction is still 1.75 percent reflectance, but the multiplicative correction is 3.15 percent reflectance (31.85/0.91 equals 35). The additive correction amount re-

TABLE 7. COMPUTED REFLECTANCES GENERATED BY USING THE HBC MODEL BASED ON IN-SITU ATMOSPHERE MEASUREMENTS (MORAN ET AL., 1992), THE DIFFERENCES BETWEEN THE COMPUTED AND AIRCRAFT-BASED GROUND-MEASURED VALUES, AND THE AVERAGE OF THE ABSOLUTE DIFFERENCES BETWEEN THESE VALUES. DOY, DAY OF YEAR, 1985-86; AVE, AVERAGE; DIFF, DIFFERENCE.

DOY (1985-86)	TM1	TM2	TM3	TM4	Ave/Diff/
204	0.0767	0.1177	0.1568	0.2236	
Diff	−0.0038	−0.0028	−0.0116	0.0081	0.0066
220	0.0732	0.1070	0.1484	0.2077	
Diff	−0.0113	−0.0186	−0.0370	−0.0173	0.0211
300	0.0778	0.0957	0.1082	0.2335	
Diff	0.0033	0.0016	0.0000	−0.0090	0.0035
300*	0.0884	0.1310	0.1782	0.2422	
Diff	−0.0069	−0.0114	−0.0165	−0.0015	0.0091
079	0.0611	0.1038	0.1427	0.2080	
Diff	−0.0087	−0.0034	−0.0112	0.0083	0.0079
095	0.0671	0.1060	0.1414	0.2102	
Diff	0.0007	0.0068	−0.0084	0.0063	0.0056
111	0.0836	0.1292	0.1833	0.2522	
Diff	−0.0088	−0.0106	−0.0228	−0.0214	0.0159
175	0.0955	0.1440	0.1977	0.2682	
Diff	−0.0091	−0.0051	−0.0124	0.0020	0.0072
Ave/Diff/	0.0066	0.0075	0.0150	0.0092	0.0096
Vegetation					
204	0.0313	0.0609	0.0367	0.5293	
Diff	0.0081	0.0020	0.0098	−0.0094	0.0073
220	0.0406	0.0594	0.0451	0.5186	
Diff	0.0104	0.0003	0.0086	−0.0675	0.0217
079	0.0264	0.0457	0.0343	0.3910	
Diff	0.0004	−0.0008	0.0041	0.0152	0.0051
095	0.0453	0.0757	0.0645	0.4030	
Diff	0.0083	0.0123	0.0112	0.0094	0.0103
111	0.0392	0.0621	0.0420	0.5837	
Diff	0.0157	0.0079	0.0181	−0.0421	0.0210
175	0.0426	0.0702	0.0492	0.5618	
Diff	0.0116	0.0052	0.0156	−0.0095	0.0105
Ave/Diff/	0.0091	0.0048	0.0112	0.0255	0.0127

*Moved from vegetation section.

TABLE 8. COMPUTED REFLECTANCES GENERATED BY USING THE IMPROVED IMAGE-BASED COSINE MODEL (COST), THE DIFFERENCES BETWEEN THE COMPUTED AND AIRCRAFT-BASED GROUND-MEASURED VALUES, AND THE AVERAGE OF THE ABSOLUTE DIFFERENCE BETWEEN THESE VALUES. DOY, DAY OF YEAR, 1985-86; AVE, AVERAGE; DIFF, DIFFERENCE.

DOY	TM1	TM2	TM3	TM4	Ave/Diff/
204	0.0747	0.1114	0.1630	0.2315	
Diff	−0.0058	−0.0091	−0.0054	0.0160	0.0091
220	0.0779	0.1112	0.1594	0.2219	
Diff	−0.0066	−0.0144	−0.0260	−0.0031	0.0125
300	0.0872	0.0994	0.1216	0.2489	
Diff	0.0127	0.0053	0.0134	0.0064	0.0095
300*	0.0970	0.1343	0.1972	0.2587	
Diff	0.0017	−0.0081	0.0025	0.0150	0.0068
079	0.0753	0.1133	0.1637	0.2337	
Diff	0.0055	0.0061	0.0098	0.0340	0.0139
095	0.0654	0.0956	0.1438	0.2035	
Diff	−0.0010	−0.0036	−0.0060	−0.0004	0.0028
111	0.0824	0.1257	0.1948	0.2719	
Diff	−0.0100	−0.0141	−0.0113	−0.0017	0.0093
175	0.0869	0.1347	0.1955	0.2667	
Diff	−0.0177	−0.0144	−0.0146	0.0005	0.0118
Ave/Diff/	0.0077	0.0094	0.0112	0.0097	0.0094
		Vegetation			
204	0.0329	0.0573	0.0379	0.5626	
Diff	0.0097	−0.0016	0.0110	0.0239	0.0116
220	0.0439	0.0622	0.0481	0.5622	
Diff	0.0137	0.0031	0.0116	−0.0239	0.0131
079	0.0420	0.0558	0.0454	0.4389	
Diff	0.0160	0.0093	0.0152	0.0631	0.0259
095	0.0473	0.0695	0.0673	0.4128	
Diff	0.0103	0.0061	0.0140	0.0004	0.0077
111	0.0352	0.0557	0.0413	0.6356	
Diff	0.0117	0.0015	0.0174	0.0098	0.0101
175	0.0336	0.0610	0.0402	0.5782	
Diff	0.0026	−0.0040	0.0066	0.0069	0.0050
Ave/Diff/	0.0107	0.0043	0.0127	0.0213	0.0123

*Moved from vegetation section.

mains the same (1.75), while the multiplicative amount again increases by 3.5 (0.9 to 3.15). Even though the increase is by a factor of 3.5 for both spectral bands, the difference in the increase in terms of percent reflectance between the 10 percent (dark) and 35 percent (bright) reflectance targets is more dramatic in the visible TM band 1 than in the near-infrared TM band 4 (7.5 and 2.25, respectively).

(3) Both of the new image-based models still ignore the effect of variations in downwelling which, according to Moran et al. (1992, p. 178), can be considerable. However, the cosine model generates results equivalent to the HBC model. There are several possible reasons for this. First, downwelling irradiance, even though it can be equal to a substantial percentage of the ground radiance (up to 25 percent according to Moran et al. (1992), p. 178), is in fact a relatively small percent of the denominator in Equation 2. The first term in the denominator is much larger than the downwelling term; therefore, the effect of downwelling is minimized. Also, in the model shown in Equation 2, the correction for the ground-to-satellite path (equal to EXP(−del*sec(TV)) in Moran et al. (1992)) was set to one because the cosine of the nadir view is equal to one; however, the values are actually slightly less than one, i.e., in the 0.85 to 0.95 range. This correction is a multiplicative coefficient in the denominator; therefore, it tends to make the denominator smaller and the reflectance value larger, while the Edown downwelling additive term makes the denominator larger and the reflectance value smaller. These two parameters, which were both ignored in my image-based models, tend to work against each other, so part of the errors associated will cancel each other out.

(4) As stated earlier, all the radiometric-correction models have the disadvantage that they are dependent on the accuracy of the system's gain and offset values. One concern is that the

sensor's characteristics change enough through time that the gain and offset values for any given image may not be accurately known. This change can cause substantial errors in the conversion of DCs to at-satellite radiances, therefore giving inaccurate reflectance values (Slater et al., 1987; Thome et al., 1993; Moran et al., in press). For multitemporal studies, a different type of radiometric correction procedure can be used to eliminate this problem. This procedure is mentioned here only to present a solution to the potential gain and offset accuracy problems encountered in all the modeling approaches discussed above. It is a hybrid method developed and used by Chavez and MacKinnon (1994) in a study dealing with automatic change detection of desert vegetation and involves making ground-reflectance measurements of a dark and bright target during a satellite overflight. The in-situ field measurements are used to apply what is called a brute force mapping of the recorded DCs directly to ground reflectances. The brute force method, which does a linear mapping of DCs to ground reflectances on the basis of ground readings, bypasses modeling corrections, so it eliminates dependence on the accuracy of the sensor's gain and offset values. A disadvantage of the method is that it requires in-situ field measurements; however, for multitemporal studies such as theirs, the hybrid method minimizes the need to be in the field during each satellite overflight. The hybrid method radiometrically corrects historical and new data to surface reflectances by slaving them onto the reflectance master using a statistical matching procedure. The sequence is (1) to radiometrically correct the one-time-only in-situ field measurements of dark and bright targets to the master image collected during the satellite overflight at the time of the ground measurements, then (2) to

TABLE 9. COMPUTED REFLECTANCES GENERATED BY USING THE IMPROVED IMAGE-BASED DEFAULT TAUs MODEL, THE DIFFERENCES BETWEEN THE COMPUTED AND AIRCRAFT-BASED GROUND-MEASURED VALUES, AND THE AVERAGE OF THE ABSOLUTE DIFFERENCE BETWEEN THESE VALUES. DEFAULT TAUz VALUES WERE 0.70, 0.78, 0.85, AND 0.91. DOY, DAY OF YEAR, 1985-86; AVE, AVERAGE; DIFF, DIFFERENCE.

DOY	TM1	TM2	TM3	TM4	Ave/Diff/
		Soils			
204	0.0926	0.1238	0.1664	0.2207	
Diff	0.0121	0.0033	−0.0020	0.0052	0.0057
220	0.0963	0.1233	0.1622	0.2110	
Diff	0.0118	−0.0023	−0.0232	−0.0140	0.0128
300	0.0786	0.0804	0.0902	0.1725	
Diff	0.0041	−0.0137	−0.0180	−0.0700	0.0265
300*	0.0874	0.1086	0.1464	0.1793	
Diff	−0.0079	−0.0338	−0.0483	−0.0644	0.0386
079	0.0777	0.1049	0.1391	0.1855	
Diff	0.0079	−0.0023	−0.0148	−0.0142	0.0098
095	0.0733	0.0962	0.1327	0.1754	
Diff	0.0069	−0.0030	−0.0171	−0.0285	0.0139
111	0.0983	0.1346	0.1914	0.2496	
Diff	0.0059	−0.0052	−0.0147	−0.0240	0.0125
175	0.1100	0.1531	0.2039	0.2598	
Diff	0.0054	0.0040	−0.0062	−0.0064	0.0055
Ave/Diff/	0.0078	0.0085	0.0180	0.0283	0.0157
		Vegetation			
204	0.0407	0.0637	0.0387	0.5363	
Diff	0.0175	0.0048	0.0118	−0.0024	0.0091
220	0.0543	0.0690	0.0489	0.5346	
Diff	0.0241	0.0099	0.0124	−0.0515	0.0245
079	0.0433	0.0517	0.0386	0.3484	
Diff	0.0173	0.0257	0.0084	−0.0274	0.0197
095	0.0530	0.0699	0.0621	0.3557	
Diff	0.0160	0.0065	0.0088	−0.0567	0.0220
111	0.0420	0.0596	0.0406	0.5834	
Diff	0.0185	0.0054	0.0167	−0.0424	0.0208
175	0.0426	0.0694	0.0419	0.5633	
Diff	0.0116	0.0044	0.0083	−0.0080	0.0081
Ave/Diff/	0.0175	0.0095	0.0111	0.0314	0.0174

*Moved from vegetation section.

radiometrically correct the historical and new image data by using a statistical histogram-matching procedure to "slave" the images onto the corrected-reflectance master image. This hybrid method makes the corrections independent of the sensor's gain and offset values, which change with time, but requires field measurements once. For historical and new data sets, the procedure becomes entirely image based and simple to apply. The need to make assumptions about overall temporal changes or brightness distribution within the image, which is required for the histogram matching phase, must be done with care. For more details on the application of the hybrid radiometric-correction procedure, see Chavez and MacKinnon (1994).

Conclusions

Two entirely image-based radiometric-correction models that are not only easy and efficent to use, but also generate results with accuracies approximately equal to those generated by the model using *in-situ* atmospheric measurements, have been presented. They are variations of the DOS model with the addition of a multiplicative correction for transmittance. The multiplicative transmittance values are derived by using mostly observed empirical relations that are straightforward and easy to apply. The COST model works well for these images, which represent a semi-arid/arid environment. However, both the cosine of the solar zenith angle and the default TAUz values seem to approximate the transmittance values given by Gilabert *et al.* (1994) for a non-arid environment and different atmospheric conditions. However, further testing is needed not only for non-arid environments and different atmospheric conditions, but also for images having higher solar zenith angles (greater than 55 degrees). As is the case with the sun-angle correction, the cosine-function correction used for the multiplicative transmittance effects by the COST model may also over-correct at higher zenith angles, so the default TAUz model will be more appropriate for those images.

Off-nadir viewing corrections are needed for images collected by either AVHRR or off-nadir viewing SPOT. The good results generated by the COST model for these data suggest that this same correction function could be considered for off-nadir viewing. The tables and scatter plots show that all models tend to overcorrect for very low reflectances (DOS the least) and that the additive scattering correction is not always the most important for the visible bands. The additive correction is more important for the darker reflectances, and the multiplicative transmittance correction is more important for brighter reflectances.

As noted by Moran *et al.* (1992), these data do not cover the full range of reflectances (TM bands 1, 2, and 3 values are generally less than 20 percent reflectance and TM 4 is greater than 20 percent). If possible, future studies should use targets that include more of the dynamic range of reflectances in all TM bands. Differences in accuracy between the visible and near-infrared bands or soils versus vegetation may actually be a bright versus dark situation.

Acknowledgments

References

Ahern, F.J., D.G. Goodenough, S.C. Jain, V.R. Rao, and G. Rochon, 1977. Use of clear lakes as standard reflectors for atmospheric measurements, *Proc. 11th International Symposium on Remote Sensing of Environment*, Ann Arbor, Michigan, pp. 731–755.

Boas, M.L., 1966. *Mathematical Methods in the Physical Sciences*, John Wiley and Sons, Inc., New York, 778 p.

Chavez, P.S., Jr., 1975. Atmospheric, solar, and M.T.F. corrections for ERTS digital imagery, *Proc. American Society of Photogrammetry Fall Conference*, Phoenix, Arizona, p. 69.

———, 1988. An improved dark-object subtraction technique for atmospheric scattering correction of multispectral data, *Remote Sensing of Environment*, 24:459–479.

———, 1989. Radiometric calibration of Landsat Thematic Mapper multispectral images, *Photogrammetric Engineering & Remote Sensing*, 55(9):1285–1294.

———, 1992. Comparison of spatial variability in visible and near-infrared spectral images, *Photogrammetric Engineering & Remote Sensing*, 58(7):957–964.

Chavez, P.S., Jr., and D.K. MacKinnon, 1994. Automatic detection of vegetation changes in the southwestern United States using remotely sensed images, *Photogrammetric Engineering & Remote Sensing*, 60(5):571–583.

Curcio, J.A., 1961. Evaluation of atmospheric aerosol particle size distribution from scattering measurement in the visible and infrared, *Journal of the Optical Society of America*, 51:548–551.

Fung, T., 1990. An assessment of TM imagery for land-cover change detection, *IEEE Transactions on Geoscience and Remote Sensing*, 28(4):681–684.

Gilabert, M.A., C. Conese, and F. Maselli, 1994. An atmospheric correction method for the automatic retrieval of surface reflectances from TM image, *International Journal of Remote Sensing*, 15(10): 2065–2086.

Hall, D.K., A.T.C. Chang, and H. Siddalingaiah, 1988. Reflectances of glaciers as calculated using Landsat-5 Thematic Mapper data, *Remote Sensing of Environment*, 25:311–321.

Hall, D.K., A.T.C. Chang, J.L. Foster, C.S. Benson, and W.M. Kovalick, 1989. Comparison of in situ and Landsat derived reflectance of Alaskan glaciers, *Remote Sensing of Environment*, 28:23–31.

Herman, B.M., and S.R. Browning, 1965. A numerical solution to the equation of radiative transfer, *Journal of Atmospheric Science*, 22:59–66.

Holm, R.G., S.M. Moran, R.D. Jackson, P.N. Slater, B. Yuan, and S.F. Biggar, 1989. Surface reflectance factor retrieval from Thematic Mapper data, *Remote Sensing of Environment*, 27:47–57.

Jackson, R.D., 1990. The MAC experiments, *Remote Sensing of Environment*, 32:77–79.

Jensen, J.R., and D.L. Toll, 1982. Detecting residential land-use development at the urban fringe, *Photogrammetric Engineering & Remote Sensing*, 48(4):629–643.

Kneizys, F.X., E.P. Shettle, L.W. Abreu, and others, 1988. *Users Guide to LOWTRAN 7*, Report AFGL-TR-88-0177, Air Force Cambridge Research Laboratories, Bedford, Massachusetts, 137 p.

Leprieur, C.E., J.M. Durand, and J.L. Peyron, 1988. Influence of topography on forest reflectance using Landsat Thematic Mapper and digital terrain data, *Photogrammetric Engineering & Remote Sensing*, 54(4):491–496.

Markham, B.L., and J.L. Barker, 1986. Landsat MSS and TM post-calibration dynamic ranges, exatmospheric reflectances and at-satellite temperatures, *EOSAT Landsat Technical Notes*, (1)3–8.

Moran, M.S., 1986. The MAC experiment, *Remote Sensing Newsletter*, University of Arizona, Tucson, (86):1–9.

Moran, M.S., R.D. Jackson, G.F. Hart, and others, 1990. Obtaining surface reflectance factors from atmospheric and view angle corrected SPOT-1 HRV data, *Remote Sensing of Environment*, 32: 203–214.

Moran, M.S., R.D. Jackson, P.N. Slater, and P.M. Teillet, 1992. Evaluation of simplified procedures for retrieval of land surface reflectance factors from satellite sensor output, *Remote Sensing of Environment*, 41:169–184.

Moran, M.S., R.D. Jackson, T.R. Clarke, J. Qi, F. Cabot, K.J. Thome, and P.N. Slater, in press. Reflectance factor retrieval from Landsat TM and SPOT HRV data for bright and dark targets, submitted to *Remote Sensing of Environment*.

Price, J.C., 1987. Calibration of satellite radiometers and the comparison of vegetation indices, *Remote Sensing of Environment*, 21: 15–27.

Robinove, C.J., P.S. Chavez, Jr., D. Gehring, and R. Holmgrem, 1981. Arid land monitoring using Landsat albedo difference images, *Remote Sensing of Environment*, 11:133–156.

Sabins, F.F., Jr., 1978. *Remote Sensing Principles and Interpretation*, Freeman, San Francisco, 425 p.

Slater, P.N., 1980. *Remote Sensing — Optics and Optical Systems*, Addison-Wesley, Reading, Massachusetts, 575 p.

———, 1985. Radiometric considerations in remote sensing, *Proc. of IEEE*, 73(6):997–1011.

———, 1988. Radiometric calibration requirements and atmospheric correction, *SPIE Proceedings*, (924):144–150.

Slater, P.N., F.J. Doyle, N.L. Fritz, and R. Welch, 1983. Photographic systems for remote sensing, *Manual of Remote Sensing, Second Edition*, American Society of Photogrammetry, Vol. 1, Chap. 6, pp. 231–291.

Slater, P.N., S.F. Biggar, R.G. Holm, and others, 1987. Reflectance- and radiance-based methods for the in-flight absolute calibration of multispectral sensors, *Remote Sensing of Environment*, 22:11–37.

Tanre, D., C. Deroo, P. Duhaut, M. Herman, J.J. Morcrette, J. Perbos, and P.Y. Deschamps, 1990. Description of a computer code to simulate the satellite signal in the solar spectrum: the 5S code, *International Journal of Remote Sensing*, 11:659–668.

Thome, K.J., D.I. Gellman, R.J. Parada, S.F. Biggar, P.N. Slater, and S.M. Moran, 1993. In-flight radiometric calibration of Landsat-5 Thematic Mapper from 1984 to present, *Proc. Society of Photo-Optical Instrument Engineering Symposium*, Orlando, Florida, pp. 126–130.

Turner, R.E., W.A. Malila, and R.F. Nalepha, 1971. Importance of atmospheric scattering in remote sensing, *Proceedings of 7th International Symposium on Remote Sensing of Environment*, Ann Arbor, Michigan, pp. 1651–1697.

Vincent, R.K., 1972. An ERTS Multispectral Scanner experiment for mapping iron compounds, *Proc. 8th International Symposium on Remote Sensing of Environment*, Ann Arbor, Michigan, pp. 1239–1247.

Forthcoming Articles